

Momentum Distributions of Isotopes Produced by Fragmentation of Relativistic ^{12}C and ^{16}O Projectiles*

D. E. Greiner, P. J. Lindstrom, H. H. Heckman, Bruce Cork, and F. S. Bieser
*Lawrence Berkeley Laboratory and Space Sciences Laboratory, University of California,
 Berkeley, California 94720*
 (Received 17 March 1975)

The fragment momentum distributions in the projectile rest frame are, typically, Gaussian shaped, narrow, consistent with isotropy, depend on fragment and projectile, and have no significant correlation with target mass or beam energy. The nuclear temperature is inferred from the momentum distributions of the fragments and is approximately equal to the projectile nuclear binding energy, indicative of small energy transfer between target and fragment.

We present here the first definitive measurements of the momentum distributions for isotopes produced by the fragmentation of heavy-ion beams at the Lawrence Berkeley Laboratory Bevatron. These results apply to the fragmentation of ^{12}C nuclei with energies 1.05 and 2.1 GeV/nucleon, and ^{16}O at 2.1 GeV/nucleon. The evaluation of the isotopic production cross sections given by Lindstrom *et al.*¹ is based on these data.

The momentum and cross-section measurements were performed with use of a single-focusing magnetic spectrometer with a half-angle acceptance of 12.5 mrad about zero degrees.² Targets were Be, CH_2 , C, Al, Cu, Ag, and Pb. The charge and mass of the fragments were obtained by measuring their rigidity (Pc/Ze), energy loss in solid-state detectors, and time of flight. Particle trajectories were determined with multiple-wire proportional chambers. The longitudinal and projected transverse momenta, P_{\parallel} and P_{\perp} , were obtained from the rigidity and direction of the particle at the focal plane of the spectrometer. The rigidity range was scanned in 0.1-GV steps from 0.8 to 10.2 GV for the 2.1-GeV/nucleon ^{12}C and ^{16}O beams and 0.2 to 6.3 GV for the ^{12}C beam at 1.05 GeV/nucleon. Because the velocities of the projectile fragments are near the beam velocity,³ these rigidity ranges allowed us to observe all particles produced having a mass-to-charge ratio, A/Z , between 0.2 and 3.4.

For each isotope the longitudinal-momentum distribution, in the projectile rest frame, was fitted by a Gaussian dependence on P_{\parallel} . The fitted variables are amplitude, central momentum, $\langle P_{\parallel} \rangle$, and standard deviation $\sigma_{P_{\parallel}}$. Figure 1 illustrates the Gaussian fit and the variables $\langle P_{\parallel} \rangle$ and $\sigma_{P_{\parallel}}$ for the case of ^{10}Be produced by the fragmentation of 2.1-GeV/nucleon ^{12}C on a Be target. The fits were restricted to the interval -400 to

+400 MeV/c which covers typically one to two decades in the magnitude of the differential cross section. The spectra of all the observed fragments exhibit properties similar to those shown in Fig. 1; namely, the momentum distributions have standard deviations of only 50–200 MeV/c, and the average momentum is slightly negative relative to the projectile.

We find that the Gaussian shape provides a good fit to the observed spectra for all isotopes regardless of beam, energy, or target except for the hydrogen isotopes. The ^2H and ^3H spectra are fitted by a Gaussian curve in the region $-300 \leq P_{\parallel} \leq 400$ MeV/c, but exhibit an enhancement for $P_{\parallel} \leq -300$ MeV/c. The ^1H spectrum cannot be fitted by a Gaussian shape in the central region $|P_{\parallel}| \leq 150$ MeV/c. In this region a fit to the ^1H spectrum is obtained with the exponential rela-

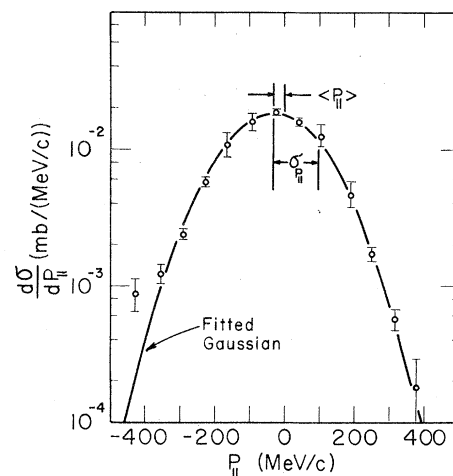


FIG. 1. The projectile-frame parallel-momentum distribution for ^{10}Be fragments from ^{12}C at 2.1 GeV/nucleon on a Be target. The mean momentum $\langle P_{\parallel} \rangle = -30$ MeV/c and standard deviation $\sigma_{P_{\parallel}} = 129$ MeV/c are indicated.

TABLE I. Momentum distribution widths and centers (MeV/c).^a

BEAM	ENERGY	SECONDARY		$\sigma_{P_{\parallel}}$	$\langle P_{\parallel} \rangle$
		Z _F	A _F		
¹⁶ O	2.10 GeV/n	1	1 ^b	71±6	-1±5
			2	134±3	-23±2
		1	3	150±3	-41±5
			3	156±2	-38±3
		2	4	131±1	-27±3
			6	167±20	-40±10
		3	6	141±7	-33±7
			7	163±4	-46±6
		3	8	170±13	-24±12
			9	188±15	-63±31
		4	7	166±2	-45±9
			9	166±7	-47±7
		4	10	159±6	-65±6
			11	197±20	-73±27
		5	8	175±22	-57±11
			10	175±7	-40±7
		5	11	160±2	-53±3
			12	163±8	-59±10
		5	13	166±10	-67±23
			10	190±9	-32±15
		6	11	162±5	-45±13
			12	120±4	-25±6
		6	13	130±3	-33±7
			14	125±3	-38±7
		6	15	125±19	-132±25
			12	153±11	-49±28
		7	13	134±2	-35±4
			14	112±3	-27±3
		7	15	95±3	-21±6
			16	54±11	-110±15
		8	13	143±14	-57±26
			14	99±6	-31±7
		8	15	94±3	-23±3
			1	67±5	0±3
		1	2	134±4	-27±3
3	138±5		-48±4		
2	3	145±8	-31±4		
	4	129±1	-25±4		
2	6	136±7	-29±15		
	6	127±7	-33±10		
3	7	144±2	-40±7		
	8	159±7	-43±12		
3	9	161±9	-35±17		
	7	145±2	-49±6		
4	9	133±3	-38±9		
	10	129±4	-30±8		
4	11	155±40	-102±82		
	8	151±16	-39±12		
5	10	134±3	-35±7		
	11	106±4	-23±9		
5	12	63±9	-96±14		
	9	147±21	-43±30		
6	10	121±6	-42±11		
	11	103±4	-40±9		
6	12	56±16	-100±11		
	1	63±4	13±4		
1	2	113±11	-13±12		
	3	162±14	-25±13		
2	3	132±14	-32±2		
	4	125±3	-27±2		
2	6	142±20	-32±14		
	6	122±10	-28±7		
3	7	142±7	-44±4		
	8	160±26	-35±14		
3	9	139±19	-43±20		
	7	140±6	-53±5		
4	9	131±9	-35±5		
	10	125±11	-37±5		
4	11	103±37	-104±43		
	8	139±12	-61±20		
5	10	135±9	-35±8		
	11	102±11	-30±4		
5	12	88±17	-112±31		
	9	147±28	-28±17		
6	10	126±8	-46±5		
	11	105±10	-43±4		
7	12	43±19	-55±19		

^aProjectile-frame parallel momentum averaged over all targets (errors include systematic and statistical contributions).

^bNon-Gaussian distribution.

tion $d\sigma/dP \propto \exp(-|P_{\parallel}|/65)$. This result applies to the protons produced within our 12.5-mrad acceptance cone and does not describe the spectra at larger production angles.

The P_{\perp} distributions, projected onto the horizontal focal plane of the spectrometer, were measured for $A \geq 2$ fragments. We find $\sigma_{P_{\perp}} = \sigma_{P_{\parallel}}$ to an accuracy of 10%, consistent with the isotropic production of these fragments.

If these reactions are examples of limiting fragmentation, the large separation in rapidity [$y = \tanh^{-1}(P_{\parallel}/E)$] between the target and the fragment distributions requires that the shape of the momentum distributions be independent of target and beam energy.⁴ For all reactions the target and energy dependence of the variables $\langle P_{\parallel} \rangle$ and $\sigma_{P_{\parallel}}$ were examined. Within the accuracy of this experiment we conclude that there is no dependence on target mass above the 5% level for $\sigma_{P_{\parallel}}$ and above the 10% level for $\langle P_{\parallel} \rangle$. Because of this observed target independence we shall refer to the target-averaged values of $\sigma_{P_{\parallel}}$ and $\langle P_{\parallel} \rangle$ in the remainder of this Letter. To determine if $\sigma_{P_{\parallel}}$ and $\langle P_{\parallel} \rangle$ are independent of energy we compare the measurements of these variables for the ¹²C beam at 2.1 and 1.05 GeV/nucleon. The weighted averages over all fragments of the quantities $\sigma_{P_{\parallel}}(2.1)/\sigma_{P_{\parallel}}(1.05)$ and $\langle P_{\parallel} \rangle(2.1) - \langle P_{\parallel} \rangle(1.05)$ are 1.02 ± 0.02 and -1.0 ± 2.0 MeV/c, respectively. This independence of beam energy and target lead to the conclusions that the ¹²C reactions satisfy the limiting-fragmentation hypothesis and the limiting-energy region is reached before 1.05 GeV/nucleon.

In the limiting-energy region the fragment distributions depend on the identity of the projectile and fragment.⁴ We begin discussion of this dependence by presenting in Table I the measured values of $\sigma_{P_{\parallel}}$ and $\langle P_{\parallel} \rangle$ for all fragments produced with sufficient signal. In Fig. 2 we have plotted the values of $\sigma_{P_{\parallel}}$ for ¹⁶O at 2.1 GeV/nucleon versus the fragment mass in atomic mass units. The charge of each fragment is used as the plotting symbol. In an attempt to parametrize the mass dependence we have fitted the data by the function $\sigma_{P_{\parallel}}^2(B, F) = 4\sigma_0^2 F(B - F)/B^2$, where B and F are the mass numbers of the beam and fragment nuclei, respectively, and σ_0 is the fitted variable. The best-fit curve for ¹⁶O is shown in Fig. 2. The fitted values of σ_0 for all beams are listed in Table II. Although the parabolic shape displays the general trend of the data, in no case does it provide a good fit to the observed values of $\sigma_{P_{\parallel}}$.⁸ The poor fit is demonstrated by

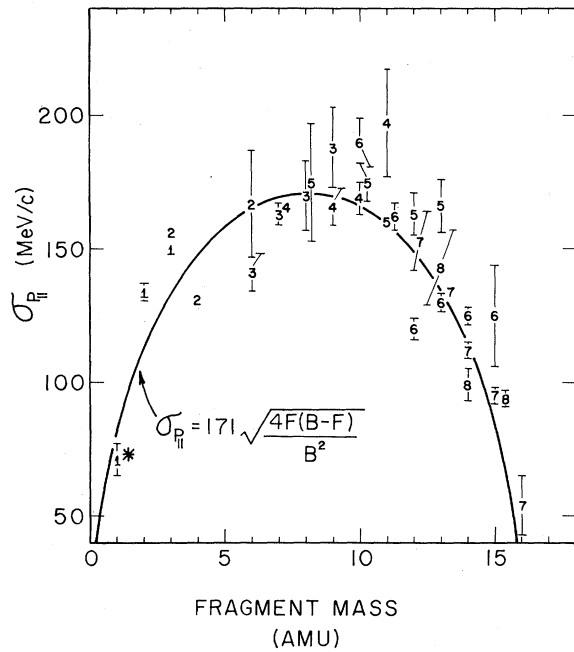


FIG. 2. Plotted are the target-averaged widths $\sigma_{P_{\parallel}}$ of the projectile-frame parallel-momentum distributions, in MeV/c, versus fragment mass in atomic mass units. The plotted symbol indicates the charge of the fragment. These data represent fragments of ^{16}O at 2.1 GeV/nucleon. The asterisk denotes that the ^1H is a non-Gaussian momentum distribution and we have used the central region of this distribution to evaluate $\sigma_{P_{\parallel}}$. This result applies to the protons produced within our 12.5-mrad acceptance cone and does not describe the spectra at larger production angles. The parabola represents the best fit to the data.

TABLE II. Comparison with theory and experiment of parameters related to a $\sigma_{P_{\parallel}}$ mass dependence of the form $\sigma_{P_{\parallel}}^2 = 4\sigma_0^2 F(B-F)/B^2$. Derived quantities are Fermi momentum $P_F = 20\sigma_0^2(B-1)/B^2$ and average excitation energy $kT = 4\sigma_0^2/m_N B$.

Parameter	Origin	Projectile		
		^{16}O 2.1 GeV/nucleon	^{12}C 2.1 GeV/nucleon	^{12}C 1.05 GeV/nucleon
σ_0 (MeV/c)	This expt.	171 ± 3	147 ± 4	141 ± 5
	Sudden approximation ^a	162	145	145
	Virtual clusters ^b	212	179	179
P_F (MeV/c)	This expt.	185 ± 3	182 ± 5	174 ± 6
	Electron scattering ^c	230	221	221
kT (MeV/nucleon)	This expt.	7.8 ± 0.3	7.7 ± 0.4	7.1 ± 0.5
Average binding energy (MeV/nucleon)	Mass measurements	8.0	7.7	7.7

^aRef. 5.^bRef. 6.^cRef. 7.

the fact that 50% of the data points are over 2 standard deviations from the curve. Particularly striking is the observation that the same complex variation of $\sigma_{P_{\parallel}}$ with fragment mass is exhibited by both the ^{12}C and ^{16}O fragments, indicating that nuclear structure effects are important variables determining $\sigma_{P_{\parallel}}$.

The values of $\langle P_{\parallel} \rangle$ have an approximately linear dependence on $\sigma_{P_{\parallel}}$ ($\langle P_{\parallel} \rangle = -0.5\sigma_{P_{\parallel}} + 30.0$ MeV/c). The general shifts in the momentum distributions toward velocities less than the beam velocity correspond to small energy transfers to the fragment, typically < 130 keV in the projectile frame. The obvious exceptions are reactions involving charge exchange, such as $^{12}\text{C} \rightarrow ^{12}\text{N}$, and charge exchange plus loss of a nucleon, e.g., $^{16}\text{O} \rightarrow ^{15}\text{C}$. The reactions involving charge exchange generally have larger negative values of $\langle P_{\parallel} \rangle \approx -100$ MeV/c. Calculation of the missing mass in these reactions gives values of approximately 200 MeV/c² after subtraction of the target mass. Thus the data are consistent with the assumption that the charge-exchange reactions proceed via pion production.

A parabolic dependence of $\sigma_{P_{\parallel}}^2$ on fragment mass of the form $\sigma_{P_{\parallel}}^2 \propto F(B-F)$, Fig. 1, was first predicted by Wenzel,⁹ later by Lepore and Riddell,⁵ and indirectly by Feshbach and Huang⁶ as extended by Goldhaber.¹⁰ In general the parabolic shape arises when one assumes (i) that the fragment momentum distributions are essentially those in the projectile nucleus, (ii) that there are no correlations between the momenta of different

nucleons, and (iii) that momentum is conserved. The validity and implications of these theories can be determined by comparison with the values of σ_0 measured by this experiment.

The work of Lepore and Riddell⁵ is a quantum mechanical calculation that employs the sudden approximation with shell-model wave functions to predict $\sigma_0^2 = \frac{1}{8} m_p B^{1/3} [45B^{1/3} - 25] (\text{MeV}/c)^2$. This expression, where m_p is the proton mass, gives qualitative agreement with the measured values as shown in Table II. Feshbach and Huang⁶ assume sudden emission of virtual clusters and relate σ_0 to the Fermi momentum of the projectile, P_F . With use of the formulation due to Goldhaber,¹⁰ the relation between P_F and σ_0 is $\sigma_0^2 = \frac{1}{20} P_F^2 B^2 / (B - 1)$. The values of P_F determined by quasielastic electron scattering⁷ give predicted values of σ_0 that are generally 25% higher than the measured values as shown in Table II. An interesting point to note here is that through the predicted relationship between σ_0 and P_F , this experiment measures the projectile Fermi momentum via nuclear fragmentation (see Table II). By assuming that the projectile has come to thermal equilibrium at an excitation temperature T , Goldhaber¹⁰ has shown that the parabolic shape is again predicted and relates σ_0 to T by the equation $kT = 4\sigma_0^2 / m_N B$, where k is Boltzmann's constant and m_N is the nucleon mass. The measured values of σ_0 then reflect excitation energies which we have listed in Table II along with the average binding energies per nucleon as determined by the projectile masses. Because

our measured excitation energies are essentially the binding energy per nucleon of the projectiles, we infer that the fragmentation process which results in bound fragments involves very little energy transfer between the target and fragment.

*Work performed under auspices of the U. S. Energy Research and Development Administration and the National Aeronautics and Space Administration, Grant No. NGR 05-003-513.

¹P. J. Lindstrom, D. E. Greiner, H. H. Heckman, B. Cork, and F. S. Bieser, Lawrence Berkeley Laboratory Report No. LBL 3650, 1975 (to be published).

²D. E. Greiner, P. J. Lindstrom, F. S. Bieser, and H. H. Heckman, Nucl. Instrum. Methods **116**, 21 (1974).

³H. H. Heckman, D. E. Greiner, P. J. Lindstrom, and F. S. Bieser, Phys. Rev. Lett. **28**, 926 (1972).

⁴W. R. Frazer *et al.*, Rev. Mod. Phys. **44**, 284 (1972).

⁵J. V. Lepore and R. J. Riddell, Jr., Lawrence Berkeley Laboratory Report No. LBL 3086, 1974 (unpublished).

⁶H. Feshbach and K. Huang, Phys. Lett. **47B**, 300 (1973).

⁷E. J. Moniz, I. Sick, R. R. Whitney, J. R. Ficenc, R. D. Kephart, and W. P. Trower, Phys. Rev. Lett. **26**, 445 (1971).

⁸Preliminary results based on eight isotopes not including ¹H indicated $\sigma_{P\parallel} \approx 140 \text{ MeV}/c$, independent of mass [H. H. Heckman, in *Proceedings of the Fifth International Conference on High Energy Physics and Nuclear Structure, Uppsala, Sweden, 1973*, edited by G. Tibbell (Elsevier, New York, 1974)].

⁹W. A. Wenzel, in Proceedings of the Lawrence Berkeley Laboratory Heavy-Ion Seminar, 1973 (unpublished).

¹⁰A. S. Goldhaber, Phys. Lett. **53B**, 306 (1974).

Production Cross Sections of Be Isotopes in C and O Targets Bombarded by 2.8-GeV α Particles: Implications for Factorization

G. M. Raisbeck and F. Yiou

Laboratoire René Bernas du Centre de Spectrométrie Nucléaire et de Spectrométrie de Masse, 91406 Orsay, France

(Received 31 March 1975)

We have measured the production cross sections of ⁷Be in C and O targets, and ⁸Be and ¹⁰Be in C targets irradiated by 2.8-GeV α particles. The results are discussed in terms of the applicability of a factorization relationship proposed for high-energy nuclear cross sections.

The availability of relativistic nuclei at synchrotrons previously devoted exclusively to proton acceleration has opened up many new possibilities for studying nuclear interactions. One of the first observations to be made from such stud-

ies was the apparent applicability of factorization to high-energy nuclear cross sections.¹ This concept, as applied by Heckman and co-workers,^{1,2} permits one to factor the fragmentation cross sections of relativistic nuclei into two parts, one